Lawrence Berkeley National Laboratory
Lawrence Berkeley National Laboratory

Title
Growth of a Au-Ni-Sn intermetallic compound on the solder-substrate interface after aging (thesis)

Permalink
https://escholarship.org/uc/item/37h7f8hj

Author
Minor, A.M.

Publication Date
1999-12-16

eScholarship.org Powered by the California Digital Library
University of California

LBNL-44758

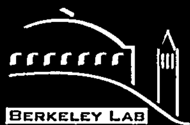

ERNEST ORLANDO LAWRENCE
BERKELEY NATIONAL LABORATORY

Growth of a Au-Ni-Sn Intermetallic Compound on the Solder-Substrate Interface After Aging

Andrew M. Minor
Materials Sciences Division

RECEIVED
APR 12 2000
OSTI

December 1999

M.S Thesis

DISCLAIMER

This document was prepared as an account of work sponsored by the United States Government. While this document is believed to contain correct information, neither the United States Government nor any agency thereof, nor The Regents of the University of California, nor any of their employees, makes any warranty, express or implied, or assumes any legal responsibility for the accuracy, completeness, or usefulness of any information, apparatus, product, or process disclosed, or represents that its use would not infringe privately owned rights. Reference herein to any specific commercial product, process, or service by its trade name, trademark, manufacturer, or otherwise, does not necessarily constitute or imply its endorsement, recommendation, or favoring by the United States Government or any agency thereof, or The Regents of the University of California. The views and opinions of authors expressed herein do not necessarily state or reflect those of the United States Government or any agency thereof, or The Regents of the University of California.

Ernest Orlando Lawrence Berkeley National Laboratory
is an equal opportunity employer.

DISCLAIMER

Portions of this document may be illegible in electronic image products. Images are produced from the best available original document.

LBNL-44758

Growth of a Au-Ni-Sn Intermetallic Compound on the Solder-Substrate Interface After Aging

Andrew Murphy Minor
M.S. Thesis

Department of Materials Science and Mineral Engineering
University of California, Berkeley

and

Materials Sciences Division
Ernest Orlando Lawrence Berkeley National Laboratory
University of California
Berkeley, CA 94720

December 1999

This work was supported by the Director, Office of Energy Research, Office of Basic Energy Sciences, Materials Sciences Division, of the U.S. Department of Energy under Contract No. DE-AC03-76SF00098.

Abstract

Growth of a Au-Ni-Sn Intermetallic Compound
on the Solder-Substrate Interface After Aging

by

Andrew Murphy Minor

Master of Science in Engineering — Materials Science and Mineral Engineering
University of California, Berkeley

Professor J.W. Morris, Jr., Chair

Au/Ni metallization has become increasingly common in microelectronic packaging when Cu pads are joined with Pb-Sn solder. The outermost Au layer serves to protect the pad from corrosion and oxidation and the Ni layer provides a diffusion barrier to inhibit detrimental growth of Cu-Sn intermetallics. As a result of reflowing eutectic Pb-Sn on top of Au/Ni metallization, the as-solidified joints have $AuSn_4$ precipitates distributed throughout the bulk of the solder joint, and Ni_3Sn_4 intermetallics at the interface.

Recent work has shown that the Au-Sn redeposits onto the interface during aging, compromising the strength of the joint. The present work shows that the redeposited intermetallic layer is a ternary compound with stoichiometry $Au_{0.5}Ni_{0.5}Sn_4$. The growth of this intermetallic layer was investigated, and results show that the ternary compound is observed to grow after as little as 3 hours at 150 °C and after 3 weeks at 150 °C has grown to a thickness of 10 μm. Additionally, methods for inhibiting the growth of the ternary layer were investigated and it was determined that multiple reflows, both with and without additional aging can substantially limit the thickness of the ternary layer.

Table of Contents

I. Introduction 1

1.1- Solder in Electronic Packaging 1

1.2- Au/Ni Metallization 2

1.3- Research on Au-Sn and Ni-Sn Intermetallics 4

II. Experimental Procedure 6

2.1- Assembly of BGA Samples 6

2.2- Microstructural Examination and Characterization 8

2.3- Microstructural Stereology 10

III. Results and Discussion 10

3.1- Determination of Ternary Compound 10

3.2- Inhibiting Growth of the Ternary Intermetallic Layer 12

3.3- Discussion of the Au-Ni-Sn System 15

IV. Conclusions and Future Work 17

V. References 18

VI. Figures 22

List of Tables and Figures

Table 1:	Common soldering alloys used in microelectronics.	2
Figure 1.1.1:	Schematic of BGA solder joint in cross-section.	22
Figure 2.1.1:	Schematic of BGA sample substrate.	23
Figure 3.1.1:	Optical micrographs of as-solidified sample.	24
Figure 3.1.2:	EDS spectrum of bulk intermetallic.	25
Figure 3.1.3:	Optical micrographs of solder/substrate interface from: a) as-solidified sample b) sample aged 3 days at 150 °C. c) sample aged 3 weeks at 150 °C.	26
Figure 3.1.4:	Optical micrographs of sample aged 3 weeks at 150 °C.	27
Figure 3.1.5:	SEM micrographs of solder-side intermetallics from: a) sample aged 3 days at 150 °C. b) as-solidified sample.	28
Figure 3.1.6:	EDS spectra of solder-side intermetallics from: a) sample aged 3 days at 150 °C. b) as-solidified sample.	29
Figure 3.1.7:	SEM images of replica debris field from aged sample.	30
Figure 3.2.1:	Plot of ternary layer thickness with aging time.	31
Figure 3.2.2:	Plot of ternary layer thickness with number of reflows.	32
Figure 3.2.3:	Plot showing the effect of aging combined with additional reflows on the thickness of the ternary layer.	33
Figure 3.2.4:	Optical micrographs of solder/substrate interface from: a) sample aged 3 days at 150 °C. b) sample aged 3 days and then reflowed again. c) sample aged 3 days, reflowed again and then aged another 3 days	34

Dedicated to

My Family-

Mom, Dad, Pat and Greg

Acknowledgements

I would first like to thank my advisor and committee chair, Professor J.W. Morris, Jr., for his support, accessibility and sharing his scientific expertise with me during my research on this thesis. Additionally, I am indebted to Professor R. Gronsky and Professor R. Maboudian for taking the time to read and approve my thesis.

From the beginning, I was lucky enough to be introduced to Dr. Zequn Mei, of the Hewlett Packard Corporation, who assisted me with my initial experimental design and subsequent results. I am additionally indebted to Rudy Bartolo, Dr. Eric Stach, Dr. Chengyu Song, and Dr. Dan Dietderich of the Lawrence Berkeley National Laboratory who assisted me with sample preparation and electron microscopy.

I was assisted throughout my research in the technical aspects of metallurgy by my many friends here in the Morris Group. Carlos Gonzalez and Ho Geon Song, particularly, were helpful with all aspects of my experimental design and interpretation. Special thanks to Chris Krenn and Dave Mitlin for their many helpful insights and for reading the first drafts of this thesis, and to Monica Barney, Koji Sato, Peter Skarpelos, Zhen Guo, Jackie Gamble, Dr. Jin Chan and Dr. Seung-Hyuk Kang for their helpful suggestions along the way.

This work was supported by the Director, Office of Energy Research, Office of Science, Division of Materials Sciences, of the U.S. Department of Energy under Contract No.DE-AC03-76SF00098.

1. Introduction

1.1 Solder in Electronic Packaging

Soldering alloys are used in microelectronics to form joints for electrical, thermal and mechanical connections between different electrical devices. The term electronic packaging refers to the hierarchical structure used to form these connections while at the same time protecting the electronic devices from environmental and mechanical damage. The most important requirements for soldering alloys used in microelectronic packaging are that the solder adequately conduct electricity and that the alloy have a low melting temperature so that the rest of the electronic device will not be harmed when the solder is melted to form the joint.

The miniaturization of microelectronics has necessitated that traditional leaded-packages be replaced by lead-less ball grid array (BGA) packages that have higher pin-to-area ratios.[1] However, BGA packaging requires that the solder joints are left as the lone structural members to hold the package together. As a result, the mechanical properties of the solder joints associated with BGA packaging have become more important than with traditional leaded and tape-automated packages.

A solder joint is actually a composite structure with a minimum of at least five different elements: the two substrates the solder is joining, the intermetallic layers that form the metallurgical bonds between the solder and the substrates, and the bulk solder itself (see Figure 1.1.1). More often, with microelectronic solder joints there are additional layers of metallization between the solder and the substrate, as well as typically more than one separate intermetallic layer, depending on the intermetallic constituents.

Eutectic Pb-Sn (38 wt.% Pb, 62 wt.% Sn) has historically been, and still is, the most widely used alloy based on its low melting temperature and good mechanical

properties compared to solders with similar melting temperatures. Other alloy systems commonly used as solders in microelectronics are listed below in Table 1:[2]

Common Soldering Alloys (wt.%), e= eutectic composition	Liquidus Temperature (°C)
48 Sn / 52 In (e)	117
42 Sn / 58 Bi (e)	138
62 Sn / 36 Pb / 2 Ag	179
62 Sn / 38 Pb (e)	183
96.5 Sn / 3.5 Ag (e)	221
99 Sn / 1 Sb (e)	235
80 Au / 20 Sn (e)	280
10 Sn / 90 Pb	302

1.2 Au/Ni Metallization

The role of metallization in solder joints is to enhance the wettability of the substrate pad, protect the pad during storage, and strengthen the solder-substrate interface after the joint is made. The conducting lines within microelectronic devices that need to be connected with solder joints are typically made of Al, Cu or an Al-Cu alloy. Both Al and Cu readily form stable oxide layers that degrade the wetting characteristics of all solder alloys. The thermodynamic driving force for wetting can be described by the well-known Young equation[3]:

If $\sigma_{sv} \geq \sigma_{lv} + \sigma_{sl}$ then the liquid will wet the solid.

Where:
- σ = surface tension
- s = solid
- l = liquid
- v = vapor

The second law of thermodynamics mandates that any spontaneous reaction such as surface oxidation must lower the the free energy associated with that system [$\partial\sigma_{sv} \leq 0$]. Therefore, oxidation or corrosion reactions that occur on substrate pads do so in order to lower the solid-vapor surface tension of that pad and consequently oxidation decreases the driving force for wetting. Thus, the ideal surface for wetting by solder alloys is a freshly-cleaned Cu surface free of oxidation, or a surface which does not readily form an oxide layer, such as Au, Pd or Pt. This is the basis on which noble metals like Au are chosen as surface finishes in microelectronic packaging.

Au finishes both maintain the wettability of the substrate pads after long-term storage and prove to have the best wetting characteristics among all traditional metallization alternatives.[4,5,6] Additionally, the high dissolution rate of Au in molten Sn (1μm/sec) and the high solubility of Au in molten eutectic Sn-Pb at 200 °C (6 wt.%)[7] leads to ultra-fast wetting of Sn-Pb on the substrate pad[8]. Au finishes are typically on the order of 1μm in thickness, so even during the fastest reflow profile all of the gold is dissolved. Upon solidification of the Sn-based solders, the Au that is dissolved from the pad metallization forms $AuSn_4$ intermetallic compounds that are densely distributed throughout the bulk of the solder as a result of the even dissolution of the Au in the molten solder.[9] Therefore, the metallurgical bond (intermetallic layer) is not formed between the Au finish and the solder, but between the solder and the metallization layer that lies beneath the Au.

The Sn-based intermetallics that form upon reflowing eutectic Pb-Sn solder on the substrate pad are without exception more brittle than either the pad metallization or the bulk solder. Therefore, while the intermetallic layer that develops at the solder-substrate interface is necessarily vital to a strong metallurgical bond (and in fact is the bond), it is ideally minimized. Cu_3Sn and Cu_6Sn_5, which are the intermetallic compounds that form when eutectic Pb-Sn solder is reflowed on Cu pads, are known to have extremely rapid growth in the solid state, having been measured to grow up to 1 μm per day at only 100 °C.[10,11]

When eutectic Pb-Sn solder is reflowed on Ni metallization, the intermetallic compound that forms at the interface is Ni_3Sn_4.[12,13] This intermetallic is extremely slow growing compared to Cu-Sn intermetallics, and provides a strong bond between the metallization and the bulk solder.[14] Additionally, the rate of Ni dissolution in molten Pb-Sn solder is extremely slow with Ni having only a negligible [13] solubility in molten eutectic Pb-Sn at 200 °C (roughly estimated at 10^{-5} at. %)[15]. Ni, therefore, provides an ideal diffusion barrier against Cu-Sn intermetallic growth when used as metallization above Cu substrate pads due to its slow rate of dissolution in molten Pb-Sn, slow consumption of Ni through intermetallic growth, and slow rate of diffusion of Cu through Ni.[16,17]

Thus, Au/Ni metallization on top of Cu substrate pads is designed to meet all of the requirements of an ideal metallization scheme. The top layer of Au provides protection from oxidation and corrosion, thus enhancing the wettability of the substrate pad even after long-term storage. The Ni intermediate layer strengthens the solder-substrate interface by forming a strong Ni_3Sn_4 intermetallic layer upon reflow, and serving as a diffusion barrier to prevent growth of Cu-Sn intermetallics in the solid-state.

1.3 Research on Au-Sn and Ni-Sn Intermetallics

Intermetallic compounds are best described as highly stoichiometric phases where small deviations in composition lead to large increases in the free energy of the system.[18] Typically, intermetallic compounds have the general form A_mB_n, where m and n are integers, and have crystal structures with low symmetry. This low symmetry typically results in poorer (more brittle) mechanical properties than those found in the constituents alone. This generalization is true of both the binary intermetallic compounds, $AuSn_4$ and Ni_3Sn_4, formed when An/Ni metallization is reflowed with eutectic Pb-Sn.[19,20]

As described in the previous section, the dissolution rates of Au and Ni in molten Pb-Sn solder are extremely different, leading to the initial formation of $AuSn_4$ intermetallics in the bulk solder, and Ni_3Sn_4 intermetallics at the solder/substrate interface. The effect of the brittleness of the Ni_3Sn_4 intermetallics at the interface is minimized due to the slow growth of the Ni_3Sn_4 layer. The low soubility of Ni in the bulk solder leads to joint properties that are essentially independent of the amount of Ni in the metallization. However, the same cannot be said of the Au content in the bulk solder.

The effect of the Au and $AuSn_4$ concentration in the bulk solder has been thoroughly documented due to a phenomenon known as gold embrittlement. Gold embrittlement refers to the observation that at relatively low gold concentrations the normally ductile Pb-Sn solder joints display brittle mechanical behavior. The maximum allowable Au concentration in a solder joint has been reported to be between 2-7 wt.%, depending on the source.[21] Additionally, it is still not clear whether the important aspect is the total Au concentration of the joint, or the distribution of Au-Sn intermetallics throughout the joint.[22] However, it has been established that gold embrittlement does degrade the shear, tensile, and creep properties of solder joints significantly.[23]

The accepted solution to the problem of gold embrittlement in joints with Au metallizations is simply to limit the thickness of the metallization so that the concentration of Au in the bulk solder is below the embrittlement limit (2 wt. %)[21]. However, this does not address problems stemming from the microstructural evolution of Au-containing joints due to solid-state aging. Two studies of solder joints reflowed on Au/Ni metallization have shown mechanical degradation of solder joints with low-Au concentrations after aging. Darveaux, *et al.*[24, 25] found that after aging near-eutectic Pb-Sn joints of 2 wt. % Au for times ranging from 50-200 hours at 150 °C, the $AuSn_4$ needles in the bulk transformed to lathlike structures, and then dissolved and reprecipitated as $AuSn_4$ at the interface. This reprecipitated intermetallic layer led to the appearance of a new failure mechanism of brittle fracture along the interface between the new $AuSn_4$ layer and the Ni_3Sn_4 layer below.

Recent research by Mei, *et al.*[26] verified the same phenomenon in joints with only 0.1 wt.% Au. They found that after extensive aging (150 °C for two weeks in their case) the $AuSn_4$ intermetallic redeposited onto the solder-substrate interface. The reconstituted interface was significantly weakened, and failed by brittle fracture along the interface between the redeposited $AuSn_4$ and the Ni_3Sn_4 layer that formed during reflow. Both the studies by Darveaux, *et al.*, and by Mei, *et al.*, used SEM EDS analysis in cross-section to confirm the redeposited intermetallic as $AuSn_4$. However, the exact mechanism for this phenomenon was not specified in either study, nor was a method of controlling this new failure mechanism discussed. Thus, the present work was undertaken to identify the mechanism of this phenomenon and explore methods for controlling it.

2. Experimental Procedure

2.1 Assembly of BGA Samples

Samples used in this study were designed to resemble ball grid array (BGA) joints typical of the current state of the art in the microelectronics industry. The BGA substrates consisted of a rigid coupon of HOFC (high oxygen free copper) with a land pattern array on one face as shown in Figure 2.1.1. The pad array was created by applying a liquid photo-imageable solder mask (EPIC 200 series) on one side of the copper coupon and then using ultraviolet photo-lithography to expose a 9 x 9 array of circular pads of 0.66 mm (26 mils) in diameter, spaced 1.27 mm (50 mils) apart.

The next step in assembling the BGA samples was applying the Ni and Au metallization layers to the underlying Cu exposed by the open circles in the solder mask. Seven different sets of substrates were made over the course of this study, in an attempt to achieve a uniform set of metallization thicknesses. Both the Ni and the Au metallizations were applied using electrolytic acid baths. The most consistent results came from applying

a current of 0.2 amps for 15 minutes to the Ni bath, and then applying a current of 30 milliamps for 8 minutes to the Au bath. These plating conditions resulted in metallization thicknesses of between 6.6 - 6.8 μm of Ni and between 1.4 - 1.5 μm of Au. The plating thicknesses were determined by cross-sectional metallography, using a digital camera and Adobe Photoshop™ digital imaging software to digitally measure the cross-sectional thicknesses.

For a given Au layer thickness, the final wt. % of Au in the solder joint could be adjusted by varying the size of the solder ball used. Assuming a perfectly dense and spherical solder ball and that the entire Au layer and none of the Ni layer was dissolved into the molten solder, the final concentration of Au in the solidified joint could be determined by using the following formula:

$$Wt.\%\,Au = \frac{m_{Au}}{m_{Solder} + m_{Au}} = \frac{t_{Au}\left(\pi r_{pad}^{2}\right)\rho_{Au}}{\left(\frac{4}{3}\pi r_{ball}^{3}\right)\left(0.62\rho_{Sn} + 0.38\rho_{Pb}\right) + \left[t_{Au}\left(\pi r_{pad}^{2}\right)\rho_{Au}\right]}$$

where: m_{Au} = mass of Au
ρ_{Sn} = density of Sn
t_{Au} = thickness of Au layer
r_{ball} = radius of solder ball

By assuming standard densities for Au, Pb and Sn,[27] joints were made with solder balls of 20 mil diameter to contain approximately 1.5 wt. % Au after reflow. Although small amounts of Ni were observed in the bulk (<< 1 at. %) with a solubility of only 10^{-5} at. % in molten solder[15] the dissolution rate of Ni in molten solder is so slow that the bulk solder can be assumed to be free of Ni.

A small amount of Kester™ mildly activated rosin flux was applied to the substrate pads before the balls were placed on the pads in order to reduce any oxide formed on the ball or pad and enhance the wetting. After placing the eutectic Pb-Sn solder balls on the pads, the samples were melted in a flowing N_2 environment following a step reflow profile with a flux activation temperature of 145 °C and then held at a peak temperature of approximately 220 °C for 10 minutes. The samples were then cooled to room temperature with liquid N_2 at a computer-controlled cooling rate of approximately 36 °C per minute.

2.2 *Microstructural Examination and Characterization*

The body of this work focused on the microstructural evolution of the interfacial layers of the solder joints during artificial solid-state aging. Joints were cross-sectioned for examination both directly after being reflowed and after being aged in a furnace at 150 °C for times of 3, 6, 12, 24, 72, 144, 216, 336, 504 and 720 hours. Additionally, combinations of pre-reflow and post-reflow aging treatments were examined, as will be discussed later.

In order to study their microstructural evolution, samples were mounted in epoxy that cures at room-temperature and then sliced with a Struers™ high speed diamond blade saw. The diamond saw was cooled by high pressure lubricant jets so as not to heat up the sample during preparation. Samples were then polished for examination using successively finer silicon carbide polishing papers from 600 down to 4000 (Struers) grit. Final polishing was performed with a combination of 3 μm colloidial diamond suspension and cerium oxide slurries of 1 μm and 0.05 μm particle size.

Microstructural examinations were made using both light-optical microscopy and scanning electron microscopy. The Nikon™ optical microscope proved especially useful through the technique of polarized light microscopy, otherwise know as Nomarski

microscopy.[28] The different constituents of the interfacial structure reflected the polarized light as different colors in cross-section, allowing for easy determination of the interfaces between layers.

The scanning electron microscopy (SEM) was performed on a 20 KeV TOPCON™ microscope equipped with an Oxford Instruments™ electron dispersive spectroscopy (EDS) detector and software. The quantitative chemical analysis discussed in this thesis was made using an internally-calibrated EDS point analysis technique, with a lateral resolution of approximately 1 μm at 20 KeV. [29]

In order to reveal the intermetallic compounds, the Pb-Sn solder was etched off of the substrate by ultrasonic agitation in a solution of glacial acetic acid and 20% H_2O_2. Approximately 90 minutes etching sufficed to remove the solder and expose the intermetallic surface on the solder side for both the aged and unaged conditions.

Further isolation of the individual intermetallic crystals was required to complete the chemical analysis, which will be described later. After etching away the Pb-Sn solder, the individual intermetallic crystals were isolated by using a replication technique commonly used in the preparation of transmission electron microscopy (TEM) samples. First, clear polymeric replication paper was dissolved onto the exposed intermetallics using acetone. After the paper dried, it was pulled off taking some of the intermetallic crystals with it. The side of the paper with intermetallics adhered to it was then coated with a fine carbon film in an Edwards™ Sputter Coater S150 B. The paper was then placed on a Cu TEM grid laced with a holey carbon film and completely dissolved using acetone. After drying, the grid was left with an amorphous carbon film containing a debris field of intermetallic crystals that could then be chemically analyzed in isolation.

2.3 Microsturctural Stereology

Measurements of various intermetallic layer thicknesses were made through cross-sectional optical microscopy. Using polarized light, the interfaces between the different layers were easily distinguished. In order to accurately measure the layer thicknesses, the images were captured using a Kodak™ digital camera, and then analyzed using Adobe Photoshop™ digital imaging software. The thicknesses of the various layers could then be measured by using a calibrated pixel/ μm conversion factor.

Each data point shown in Figures 3.2.1 through 3.2.3 represents 90 different measurements. For each aging and reflow condition analyzed, there were 9 different solder joints cross-sectioned for examination. From each of these different joints there were two pictures taken digitally, and from each picture there were five measurements taken from standard positions within each picture. This method gave a small standard error (standard deviation/ (number of measurements)^0.5) and represented an objective calculation of thicknesses. For example, the data points for Fig. 3.2.1 had standard deviations ranging between 20% and 40%, and standard errors ranging between 7.8% and 22.5%.

3. Results and Discussion

3.1 Determination of Ternary Compound

The as-solidified joints contained dense distributions of small needle-like $AuSn_4$ intermetallics evenly dispersed throughout the bulk, as seen in Figure 3.1.1. The interface between the Ni metallization layer and the bulk solder joint contained a thin layer of Ni_3Sn_4 intermetallic, as identified by SEM EDS analysis. The Ni_3Sn_4 layer is difficult to view in cross-section with the optical microscope due to its small thickness of approximately 0.5 μm. EDS analysis showed that the $AuSn_4$ intermetallics in the bulk were essentially

devoid of Ni, while the Ni_3Sn_4 intermetallic at the interface contained very little measurable Au in the unaged condition. An EDS spectrum from the bulk $AuSn_4$ intermetallic is shown in Figure 3.1.2, and the determination of the Ni_3Sn_4 layer by EDS analysis will be described below.

As illustrated in Figure 3.1.3, a coarse intermetallic layer develops above the Ni_3Sn_4 layer as the sample is aged. Figures 3.1.3 (a),(b), and (c) show cross-sections of samples as-solidified, aged for 3 days, and aged for 3 weeks, respectively. Figures 3.1.3 b and c show a coarse intermetallic layer above the Ni_3Sn_4 and Ni metallization layers (although the Ni_3Sn_4 layer is too small to be seen here). This intermetallic layer can be seen after as little as 3 hours of aging at 150 °C, and has reached 10 μm thickness after three weeks at 150 °C. As can be seen in Figure 3.1.1, before aging the intermetallics are distributed throughout the joint, including near the solder/substrate interface. Figure 3.1.4 shows the distribution of $AuSn_4$ intermetallics in the bulk of the solder after aging. After the joints were aged, the side of the joint nearest the interface became essentially depleted of $AuSn_4$ intermetallics. The simultaneous depletion of $AuSn_4$ from the bulk solder nearest the interface and the growth of the new intermetallic layer suggests that this intermetallic layer forms by the reconfiguration of the Au-Sn, as found also by Mei, *et al.* [26]

In order to determine the composition of the coarsened intermetallic, the Pb-Sn solder was etched off of the substrate by ultrasonic agitation in a solution of glacial acetic acid and 20% H_2O_2. The appearance of the revealed interfaces after etching for both the as-soldered and aged samples is shown in Figure 3.1.5. The composition of the exposed surface was then measured with SEM EDS.

In Figure 3.1.6, the EDS spectra from the solder-side intermetallic layer of an as-solidified sample (a) is compared to that of a sample aged for 3 days at 150 °C, (b). The intermetallic in the as-solidified sample has a nominal composition of Ni_3Sn_4, with 1.4 at. % residual Au. The intermetallic in the aged sample has a Au content of 10 at. %, and a composition close to $Au_{0.5}Ni_{0.5}Sn_4$. It thus appears that the reprecipitated intermetallic is

a Au-Ni-Sn ternary compound, and not simply the redeposition of the binary $AuSn_4$ intermetallic from the bulk solder. This is a new result which is contrary to the previous observations of Darveuaux, *et al.* [24,25] and Mei, *et al.*[26].

The ternary intermetallic does not form during initial soldering since the high solubility of Au in the molten solder causes the Au to dissolve, separating it from the Ni. The subsequent reconfiguration to the interface is a consequence of the availability of Ni there.

To confirm this composition, and eliminate the possibility of spurious readings from a mixture of intermetallics, extraction replication was used to remove individual crystals from the redeposited intermetallic layer. Figure 3.1.7 shows the debris field of the replica crystals on a Cu TEM grid. Unfortunately, the crystals of approximately 1 μm in thickness were not electron-transparent under a 200kV transmission electron microscope, but EDS spectra taken from this grid with the SEM verified that the crystals were indeed ternary Au-Ni-Sn intermetallic compounds.

3.2 *Inhibiting Growth of the Ternary Intermetallic Layer*

As described by Mei, *et al.*[26], the growth of the new intermetallic compound on the interface after aging has severe consequences on the mechanical integrity of an aged solder joint. Their study found that the aged joints failed through brittle fracture in four-point bend tests between the newly redeposited intermetallic layer and the Ni_3Sn_4 layer. The aged joints were found to be significantly weaker than the same joints tested before aging. Therefore, a goal of this study was to investigate methods that would inhibit the growth of the ternary $Au_{0.5}Ni_{0.5}Sn_4$ layer during aging.

Figure 3.2.1 shows a plot of the thickness of the redeposited $Au_{0.5}Ni_{0.5}Sn_4$ layer with aging time at 150 °C. It can be seen that the growth of the ternary layer varies roughly as $t^{0.4}$, where t is the aging time. This is expected since the growth is dependent on both

the bulk diffusion of Au towards the solder/substrate interface (varying as $t^{0.5}$) and the diffusion-controlled precipitate coarsening (typically varying as $t^{0.3}$)[30]. In addition to the increased thickness of the ternary intermetallic seen after significant aging, the interface between the intermetallic and the bulk solder is observed to become smoother, which is expected from the thermodynamic driving force favoring the minimization of surface area. This observation is significant since it is known that a smooth intermetallic/solder interface as opposed to a rough surface degrades the mechanical properties of the joint due to the decreased resistance to shear along the interface.[31]

Two methods were determined in this study that reduce the thickness of the redeposited ternary layer after aging. The first method is illustrated in Figure 3.2.2, where it can be seen that the thickness of the redeposited layer decreases substantially if the samples are processed with multiple reflows before aging.** The samples that underwent more than one reflow had decreased ternary intermetallic thicknesses of approximately 30-50% compared to the samples that underwent only one reflow prior to aging, as seen in Figure 3.2.2.

The exact mechanism for why the time spent in the molten state has an effect on the growth of the ternary intermetallic layer during subsequent solid-state aging is not known, however one observation leads to a possible explanation. It was observed that in some of the samples undergoing multiple reflows prior to aging, the thickness of the Ni_3Sn_4 layer was slightly larger than in the samples only undergoing one reflow prior to aging. Essentially, multiple-reflows increase the amount of time spent above the solidus point of 183 °C for eutectic Pb-Sn solder, as each reflow brings the joints to a peak temperature of 220 °C for approximately 5 minutes. If the Ni_3Sn_4 layer acted as a barrier to the diffusion of Ni from the Ni metallization layer below, then the source of Ni for the growth of the $Au_{0.5}Ni_{0.5}Sn_4$ layer during solid-state aging would be decreased with a thicker Ni_3Sn_4 layer.

** In this case each reflow is the same as the first, where the solder is completely melted. It is also common in the microelectronics industry to refer to multiple reflows where only the first reflow melts the solder alloy, and all subsequent reflows take the joint near, but not above the solder liquidus temperature.

As an extension to this hypothesis, a second method for inhibiting the growth of the ternary layer was determined. Figures 3.2.3 and 3.2.4 show the effects of additional reflows after aging, as opposed to before aging. It was found that reflowing a joint that had been aged for 3 days caused the redeposited $Au_{0.5}Ni_{0.5}Sn_4$ layer to spall off of the interface. If the reflowed joint was then aged for another 3 days, the intermetallic growth was much less pronounced. These results are consistent with the hypothesis that the enlarged Ni_3Sn_4 layer partially acts as a barrier to the diffusion of Ni. The state of the $Au_{0.5}Ni_{0.5}Sn_4$ intermetallics that spalled off of the interface during the post-aging reflow was not investigated, and so it is not known whether they remelted or remained stable in the molten bulk solder.

Thus, a combination of post-aging reflows and additional aging has the same effect of inhibiting the growth of the ternary layer as does multiple reflows prior to aging. This finding is contrary to the popular belief that limiting the time spent in the molten stage during joint assembly leads to stronger joints.[32] This common belief arises from the importance in limiting the growth of intermetallics, which is accelerated at high temperatures where the bulk solder is molten. However, if a manufacturer is concerned with the mechanical integrity of their solder joints when using the system investigated here, then longer time spent in the molten stage of the joint reflow process would be beneficial. In this case, the thickened Ni_3Sn_4 intermetallic that results from holding the joints above the solder melting temperature for a long time actually decreases the thickness of the combined intermetallic layers over time.

An additional method for inhibiting the growth of the ternary layer is proposed here, but was not investigated in this study. The proposed method is to minimize the thickness of the Au metallization so that its concentration in the solder remains well below the solubility limit (~0.3 wt. %)[7]. For example, Blair *et al.* [33] aged eutectic Pb-Sn joints on Au/Ni substrates at 160 °C for up to 36 days, without noticeable precipitation of a Au-Ni-Sn intermetallic layer. Their samples had a Au metallization layer of only 0.127 μm and

solder balls .55g in weight; hence the maximum possible concentration in their solder was well below the 0.3 wt. % solubility limit of Au in eutectic Pb-Sn solder.*

3.3 Discussion of the Au-Ni-Sn System

The $Au_{0.5}Ni_{0.5}Sn_4$ phase has not been mentioned in any thermodynamic study of the ternary Au-Ni-Sn system. A 400 °C section of the Au-Ni-Sn ternary phase diagram reported by Neumann, *et al.* [34] does include the ternary intermetallic $AuNi_2Sn_4$, which is a substitutional variant of Ni_3Sn_4. Their study also includes a determination of the crystallographic space group of $AuNi_2Sn_4$, a phase which had never been seen before. However, a room temperature section of the Au-Ni-Sn ternary phase diagram compiled by Anhock, *et al.* [35] using SEM EDS analysis does not mention any ternary compounds, but describes high mutual solubility of Ni and Au in each other's Sn-based intermetallic compounds. This room temperature ternary section by Anhock, *et al.* was compiled from EDS data only, and verification of the phases by crystallographic means was not achieved. Thus, it seems plausible that a stable ternary phase might have been interpreted as a binary phase with a high solubility of a third component.

Confirmation of the $Au_{0.5}Ni_{0.5}Sn_4$ phase as the newly redeposited phase in this system came in a study by A. Zribi, *et al.*,[36] during the publication of this present work. Zribi, *et al.* studied the effect of aging at 150 °C on eutectic Pb-Sn joints of approximately 0.2% Au resulting from the standard Au/Ni metallization. They also determined by SEM-EDS the redeposited phase to be of stoichiometry $Au_{0.5}Ni_{0.5}Sn_4$, but did not provide crystallographic data to support the new phase.

---

* Assuming a worst-case scenario of a hemispherical cap of solder with a radius equal to the original ball diameter, the solder joint would have a Au wt. % of 3.4×10^{-4}.

While the crystal structure of the new phase remains to be determined, the composition $Au_{0.5}Ni_{0.5}Sn_4$ suggests that the redeposited phase is a variant of $AuSn_4$ with 50% Ni substitution for Au. It is, apparently, thermodynamically preferred to $AuSn_4$ in this system, which explains its gradual growth during aging in the solid state.

4. Conclusions and Future Work

The present work examined an intermetallic phase that had been reported to redeposit on the solder/substrate interface after aging eutectic Pb-Sn solder joints reflowed on Au/Ni metallization. It was determined that the redeposited phase was not binary $AuSn_4$, as had been reported previously, but actually a ternary compound with stoichiometry $Au_{0.5}Ni_{0.5}Sn_4$. The growth of this intermetallic layer was investigated, and results show that the ternary compound was observed to grow after as little as 3 hours at 150 °C, and after 3 weeks at 150 °C had grown to a thickness of 10 μm. Additionally, methods for inhibiting the growth of the ternary layer were investigated, and it was determined that multiple reflows, both with and without additional aging can substantially limit the thickness of the ternary layer.

Further study of this new ternary compound would include a determination of the crystallographic space group that would help determine whether $Au_{0.5}Ni_{0.5}Sn_4$ is an entirely new phase, or a compositional variant of a prior-known phase such as $AuNi_2Sn_4$. Additionally, further study of the multiple-reflow effect prior to aging would help to refine methods for limiting the redeposition of the ternary layer. A full understanding of the redeposition of $Au_{0.5}Ni_{0.5}Sn_4$ and the methods for controlling it would enhance the reliability of Au/Ni metallization in BGA microelectronic packages, and would help lead to more reliable microelectronics in the future.

[1] J. Lau, Ball Grid Array Technology, McGraw Hill, Inc.,NY (1995) p.36

[2] J. Hwang, Modern Solder Technology for Competitive Electronics Manufacturing, McGraw Hill, Inc., NY (1996) pp.59-63

[3] Morris Jr., J.W., *Lecture Notes for MSME 201A- Thermodynamics*, University of California, Berkeley, Fall 1997, p. 270

[4] F.H. Reid and W. Goldie, Gold Plating Technology, Electrochemical Publications Limited, Palo Alto, CA (1974) p.226

[5] G.A.Walker and P.W. DeHaven, "Initial Wetting and Reaction Sequences in Soldering", *IEEE International Reliability Physics Symposium*, (1984) p.181

[6] E. Bradley and K. Banerji, "Effect of PCB Finish on the Reliability and Wettability of BallGrid Array Packages," *IEEE Trans. on Compon. Packag. Manuf. Tech. B. Adv. Packag.* ,**19** no.2 (1995) p.1028

[7] A. Prince, "The Au-Pb-Sn Ternary System", *J. Less Common Metals*, **12** (1967) pp.107-116

[8] P.G. Kim and K.N. Tu, "Morphology of wetting reaction of eutectic SnPb solder on Au foils", *J. Appl. Phys.*, **80** no.7 (1996) p.3822

[9] P.G.Kim and K.N Tu,"Fast dissolution and soldering reactions on Au foils", *Mat. Chem.and Phys.*, **53** (1998) pp.165-171

[10] J.D. Demaree, "Growth Rate of Solder Intermetallics", (Materials Synthesis and Processing Using Ion Beams Symposium, Boston, MA, Nov. 1993),*Mater. Res. Soc.*, (1994) p.801

[11] A. So, Y. Chan and J.K.L. Lai, "Aging Studies of Cu-Sn Intermetallic Compounds in Annealed Surface Mount Solder Joints," *IEEE Trans. on Compon. Packag. Manuf. Tech.-B.*, **20**, no.2, (1997) p.161

[12] T.B.Massalski,ed.,Binary Alloy Phase Diagrams, American Society for Metals, Metals Park, Ohio, (1986) p.1759

[13] G. Ghosh, "Thermodynamic Modeling of the Ni-Pb-Sn System", *Met. Trans*., **30A**, (1999) p.1481

[14] A.Rahn, The Basics of Soldering, John Wiley and Sons, Inc.,NY (1993) p.28

[15] A. Zribi,R. Chromik, R. Prethus, J.Clum, K. Teed, L. Zavalij, J. Devita, J.Tova and E.J. Cotts "Solder Metallization Interdiffusion in Microelectronic Interconnects", *IEEE Electronic Components and Technology Conference*, (1999) p. 451

[16] H. Keller, "Solder Connections with a Ni Barrier", *IEEE Electronic Components Conference Proceedings*, (1986) p.31

[17] W. Yujing, E. Jacobs, C. Pouraghabagher and R. Pinizzotto, "In-Situ TEM Study of Copper-Tin Intermetallic Formation", *Mat. Res. So. Syump. Pro.* **323**, (1994) p.165

[18] D. Porter and K. Easterling,Phase Transitions in Metals and Alloys, 2nd. ed., Champman &Hall, London, (1992) p.27

[19] D.H. Daebler, "Overview of Gold Intermetallics in Solder Joints", *Surface Mount Technology*, October (1991), p.43

[20] D.R. Frear, J.R. Michael and P.F. Hlava, "Analysis of the Reaction between 60Sn-40Pb Solder with a Pd-Pt-Ag-Cu-Au Alloy", *J. of Elect.Mater.*, **22**, no.2, (1993)p.185

[21] M. Ferguson, C. Fieselman and M. Elkins, "Manufacturing Concerns When Soldering with Gold Plated Component Leads or Circuit Board Pads", *IEEE Trans. on Compon. Packag. Manuf. Tech.-C*, **20**, no.3, (1997) p.188

[22] P. Kramer, J. Glazer, and J.W. Morris, Jr., "The Effect of Low Gold Concentrations on the Creep of Eutectic Tin-Lead Joints", *Met. Trans*., **25A**, (1994) p.1249

[23] P. Kramer, "The Effect of Low Au Concentrations on the Properties of Eutectic Sn/Pb", M.S. Thesis, U.C. Berkeley, (May 1992)

[24] R.Darveaux, K. Banerji, A. Mawer, and G. Dody, Ball Grid Array Technology, edited by John Lau, McGraw-Hill, NY, (1995) pp. 379-442

[25] Banerji K., R. Darveaux, "Effect of the Aging on the Strenght and Ductility of Controlled Collapse Solder Joints",*Proc. of the TMS-AIME First Int'l Conf. on Microstructure and Mechanical Properties of Aging Materials*, (1992) pp.431-442

[26] Z. Mei, A. Eslambolchi and P. Johnson,"Brittle Interfacial Fracture of PBGA Packages Soldered on Electroless Nickel/ Immersion Gold", *Proc. of the 48th Electronic Components and Technology Conf., IEEE*, (1998) p.952

[27] R. Weast, ed., CRC Handbook of Chemistry and Physics, CRC Press, Boca Raton, FL, (1985) pp. B 68-161

[28] D. Lessor, J. Hartman, and R. Gordon, "Quantative surface topography determination by Nomarski reflection microscopy", *J. of Opt. Soc. of America*, **69** no.2 (1979) pp. 357-366

[29] D. Williams and C.B. Carter, Transmission Electron Microscopy, Plenum Press, NY, (1996) p. 632

[30] J. Martin, R. Doherty and B. Cantor, Stability of Microstructure in Metallic Systems, Cambridge Univ. Press, NY, (1997) p.271

[31] Y. Chan, P. Tu, A. So, and J. Lai, "Effect of Intermetallic Compounds on the Shear Fatigue of Cu/63Sn-37Pb Solder Joints", *IEEE Trans. on Compon. Packag. Manuf. Tech. -B*, **20** no.4 (1997) p.463

[32] J. Hwang, Modern Solder Technology for Competitive Electronics Manufacturing, McGraw Hill, Inc., NY (1996) p.387

[33] H.D. Blair, T. Pan and J.M. Nicholson,"Intermetallic Compound Growth on Ni, Au/Ni, and Pd/Ni Substrates with Sn/Pb, Sn/Ag, and Sn Solders", *Proc. of the 48th Electronic Components and Technology Conf., IEEE*, (1998) p.259

[34] Neumann, A. , A. Kjekshus and E. Røst, "The Ternary System Au-Ni-Sn", *J. Solid State Chemistry*, (1996) **123** p.203

[35] Anhock, S., H. Oppermann, C. Kallmayer, R. Aschenbrenner, L.Thomas, H.Reichl,"Investigation s of Au/Sn alloys on different end-metallizations for high temperature applications", *Proc. of the IEEE/CPMT Berlin Int'l Electronics Manufacturing Technology Symposium*, (1998), p.156

[36] A. Zribi, R. Chromik, R. Prethus, J. Clum, L. Zavalij, and E. Cotts, "Effect of Au-Intermetallic Compounds on the Mechanical Reliability of Sn-Pb/ Au-Ni-Cu Joints",*InterPACK Conf., Advances in Electronic Packaging*, **26** no.2 (1999) p.1573

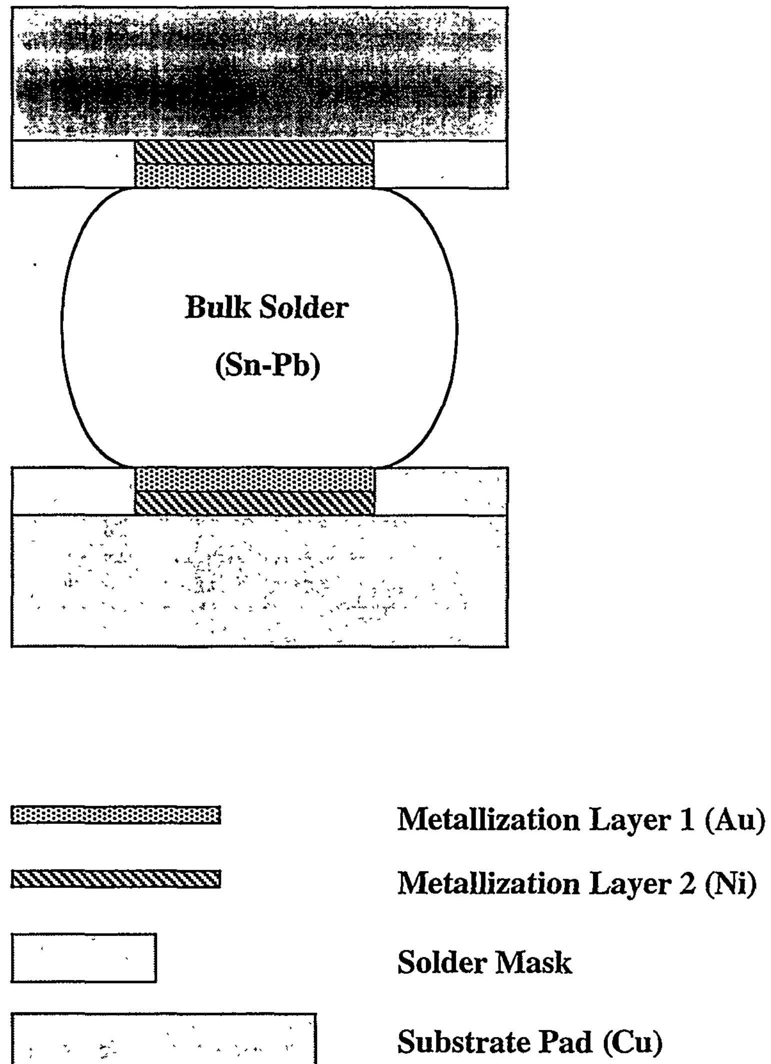

Figure 1.1.1- Schematic of BGA solder joint cross-section before reflow. (Metals used in this study in parentheses)

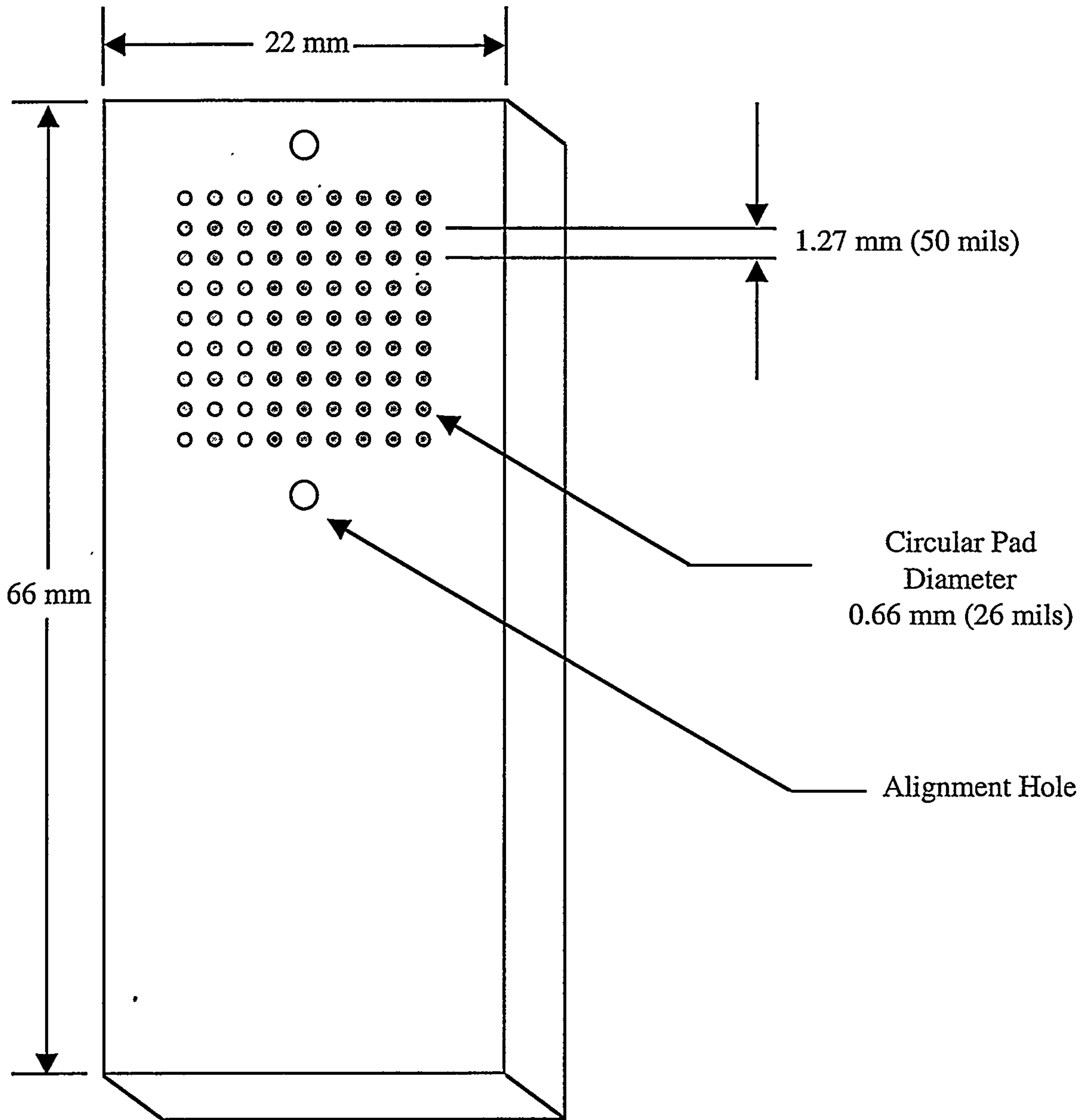

Figure 2.1.1- Schematic Illustration of BGA Sample

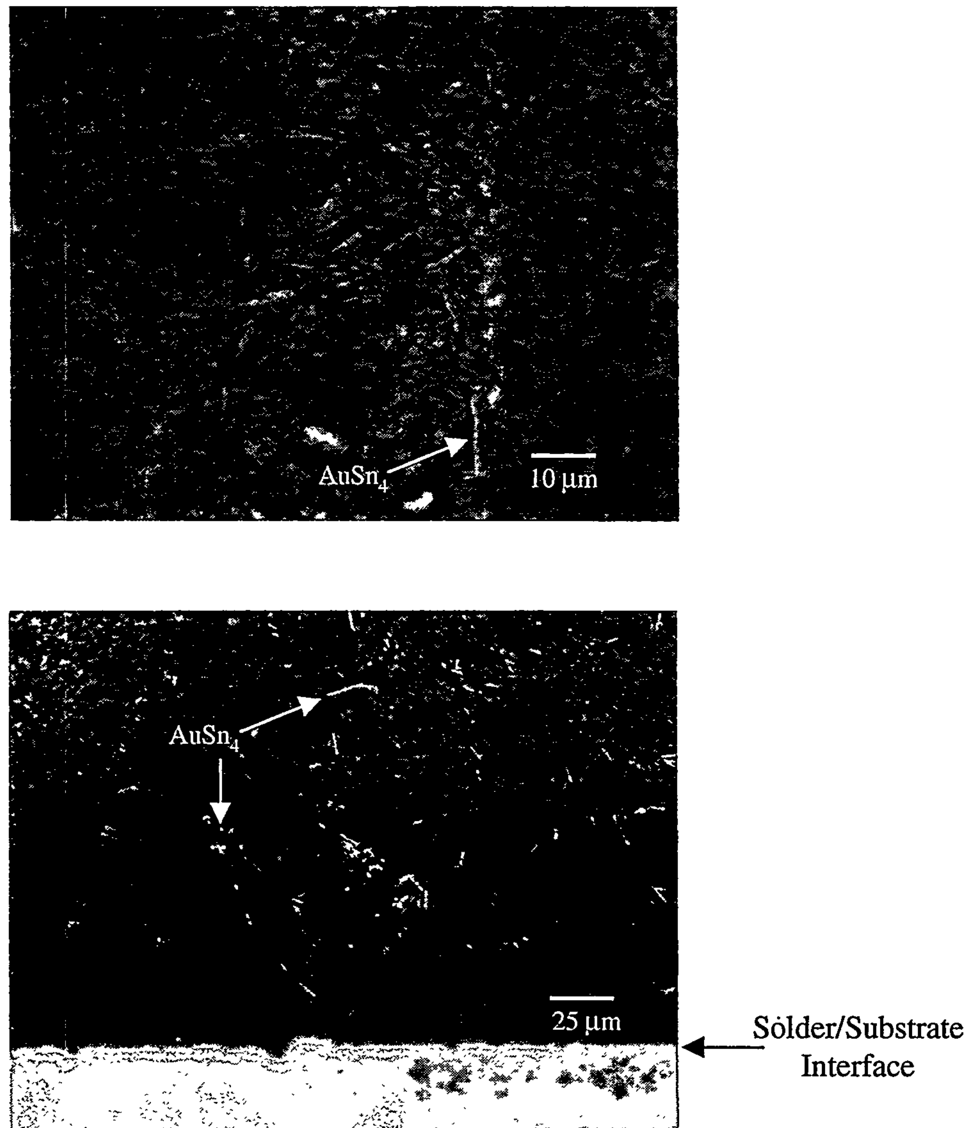

Figure 3.1.1- Optical micrograph of as-solidified sample etched to show distribution of $AuSn_4$ intermetallics in bulk.

Top: 1000X magnification.
Bottom: 400X magnification

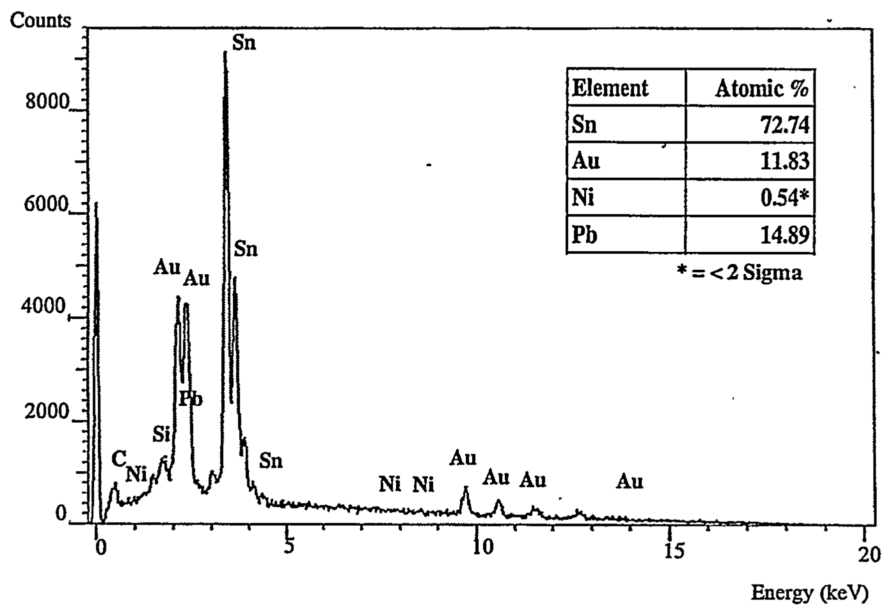

Element	Atomic %
Sn	72.74
Au	11.83
Ni	0.54*
Pb	14.89

Figure 3.1.2- EDS spectrum of the bulk intermetallic from the as-solidified sample showing no presence of Ni. (Note: the Pb content comes from the bulk solder and the Si peak is an artifact of the silica suspension polishing fluid)

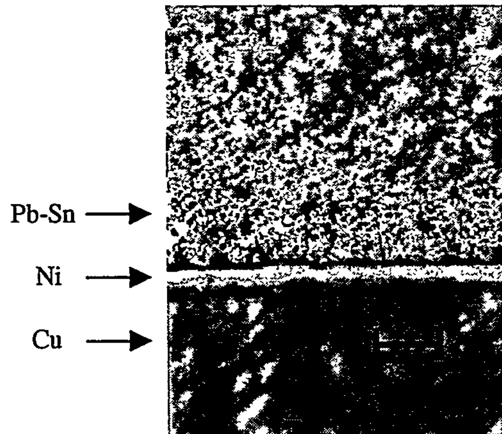

Figure 3.1.3a- Cross-section of as-solidified sample showing no Au-Ni-Sn layer.

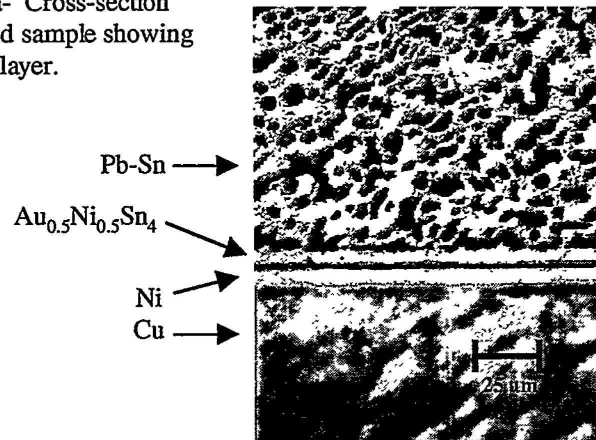

Figure 3.1.3b- Cross-section of sample aged 3 days at 150 °C showing a ~ 4μm Au-Ni-Sn layer.

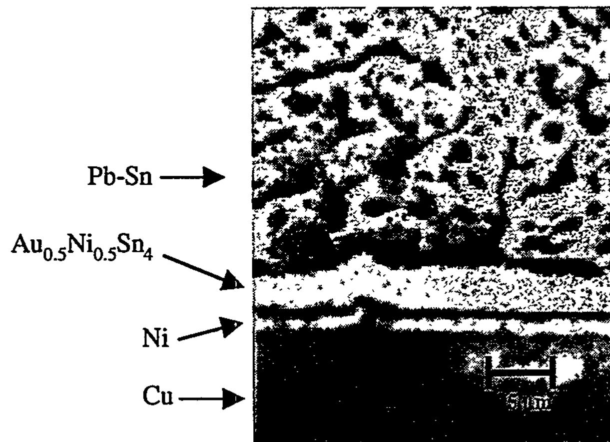

Figure 3.1.3c- Cross-section of sample aged 3 weeks at 150 °C showing a ~ 10μm Au-Ni-Sn layer.

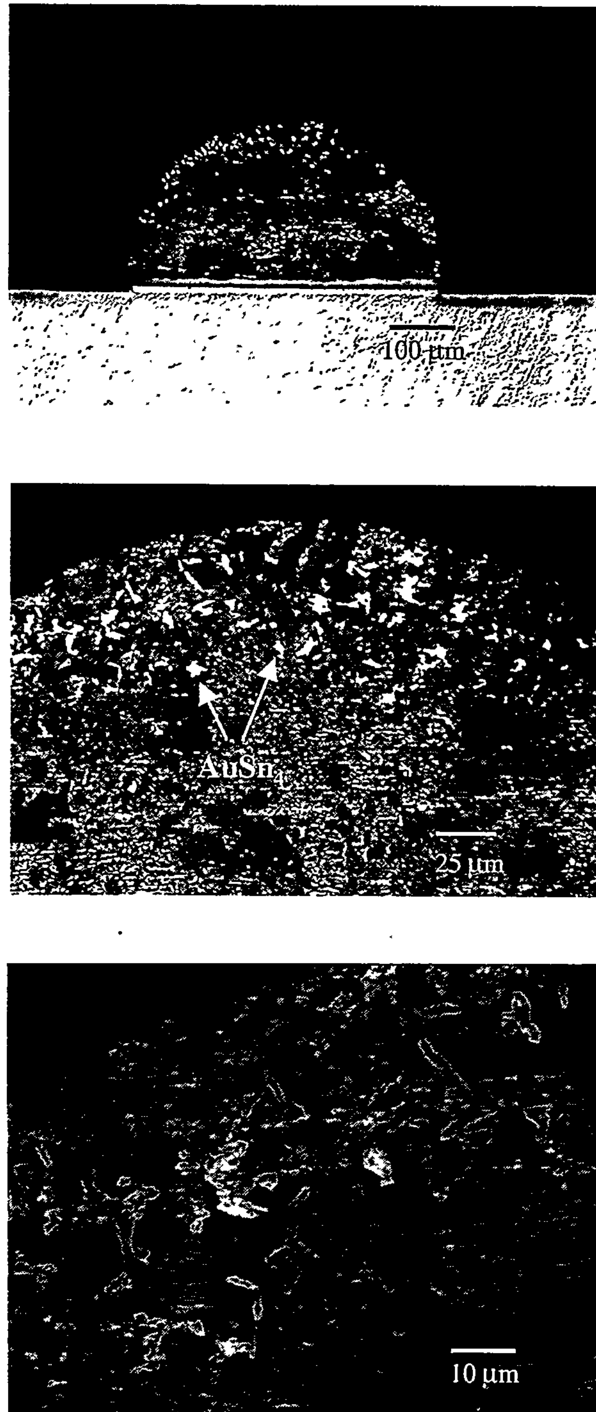

Figure 3.1.4- Optical micrograph of sample aged 3 weeks at 150 °C etched to show distribution of $AuSn_4$ intermetallics only in farthest part of the bulk from the solder.
Top: 100X magnification.
Middle: 400X magnification
Bottom: 1000X magnification

Figure 3.1.5a- SEM picture of $Au_{0.5}Ni_{0.5}Sn_4$ intermetallic crystals with Pb-Sn solder etched off. Replica samples were made of the individual crystals seen above.

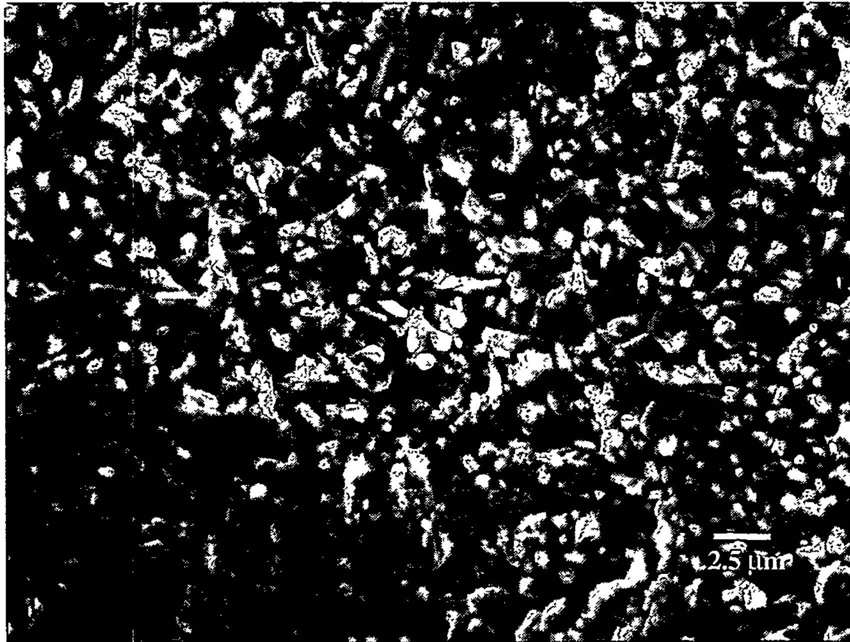

Figure 3.1.5b- SEM picture of Ni_3Sn_4 intermetallic crystals with Pb-Sn solder etched off.

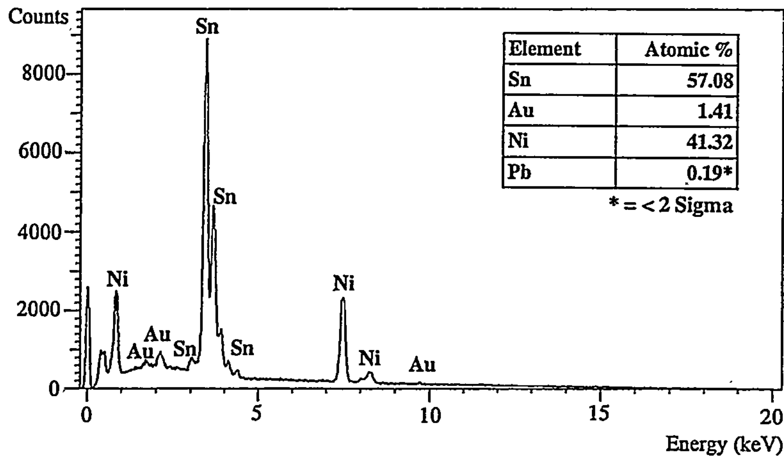

Figure 3.1.6a- EDS spectrum of the solder-side intermetallic from the as-solidified sample. The quantitative elemental analysis shows the intermetallic has a composition of Ni_3Sn_4.

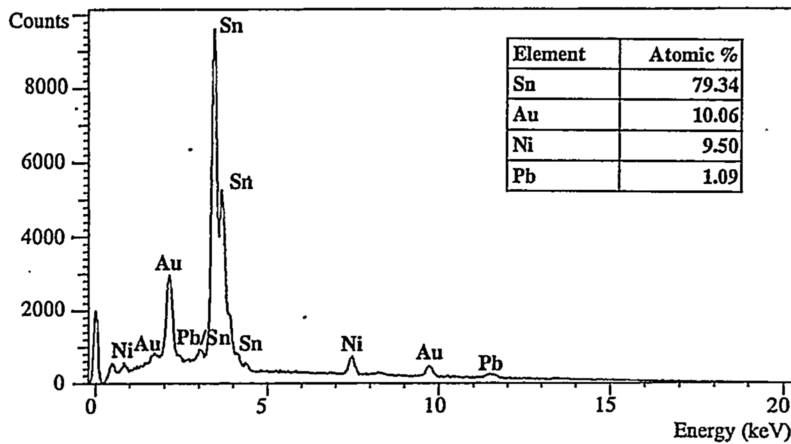

Figure 3.1.6b- EDS spectrum of the solder-side intermetallic from the sample aged 3 days at 150 °C. The quantitative elemental analysis shows the intermetallic has a composition of $Au_{0.5}Ni_{0.5}Sn_4$.

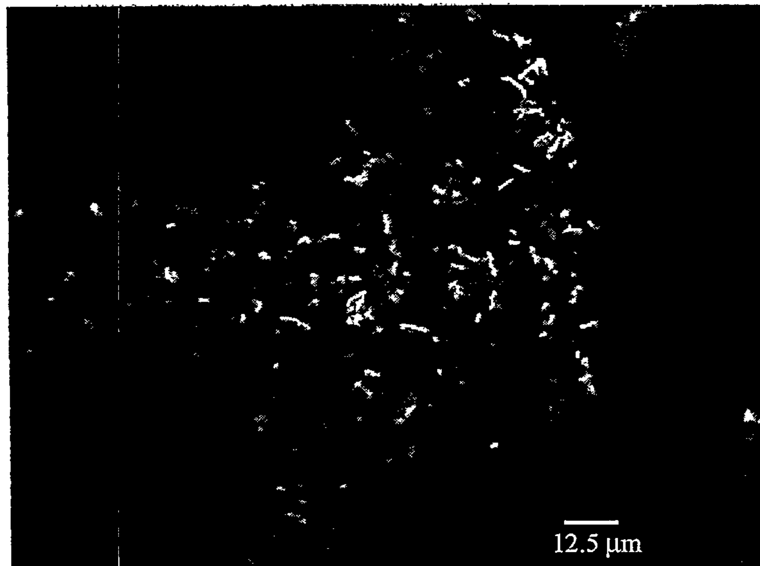

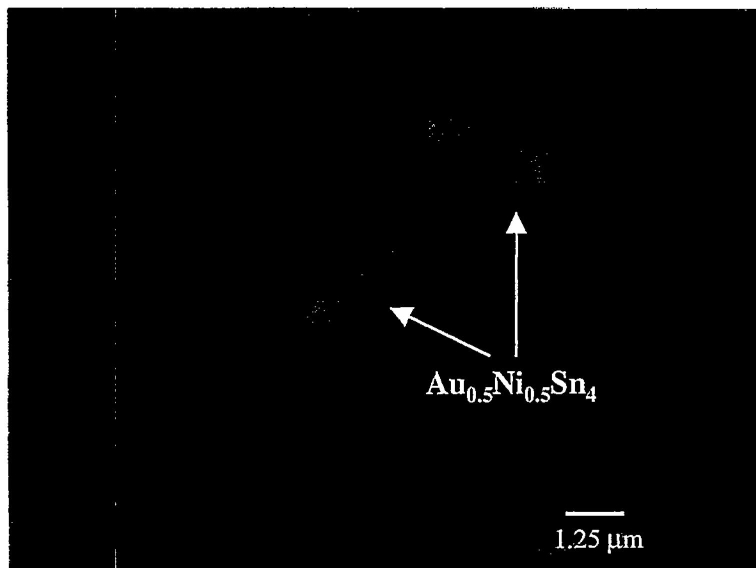

Figure 3.1.7- SEM images of replica debris field on Cu TEM grid from sample aged 3 days at 150 °C.

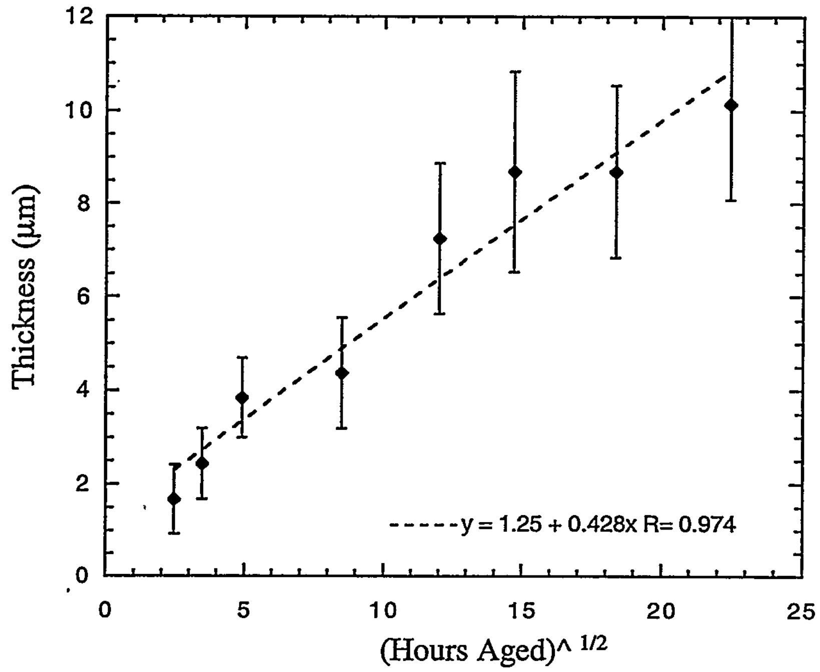

Figure 3.2.1- Thickness of the $Au_{0.5}Ni_{0.5}Sn_4$ intermetallic layer with the square root of aging time at 150 °C. (Error bars represent one standard deviation.)

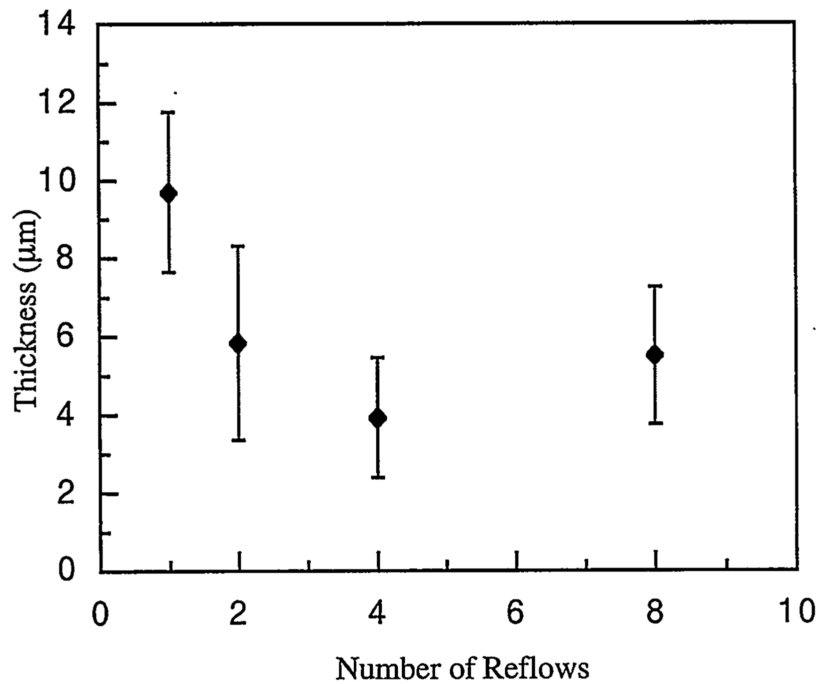

Figure 3.2.2- Thickness of $Au_{0.5}Ni_{0.5}Sn_4$ intermetallic layer with the number of reflows prior to aging for 30 days at 150 °C. (Error bars represent one standard deviation.)

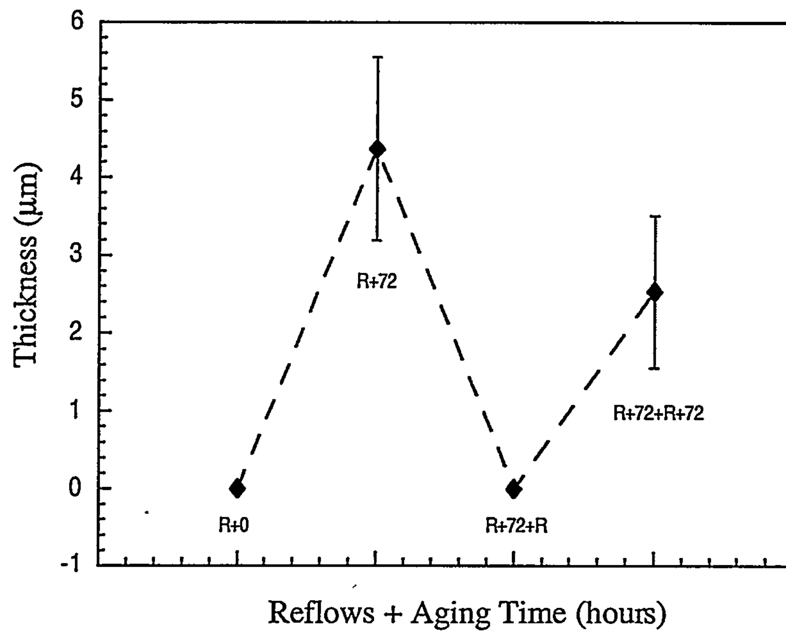

Figure 3.2.3- Effect of aging at 150 °C and additional reflows on $Au_{0.5}Ni_{0.5}Sn_4$ intermetallic layer. (Error bars represent one standard deviation.)

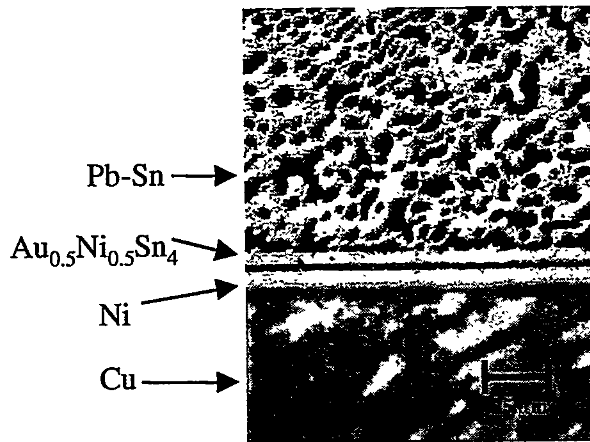

Figure 3.2.4a- Sample aged 3 days at 150 °C

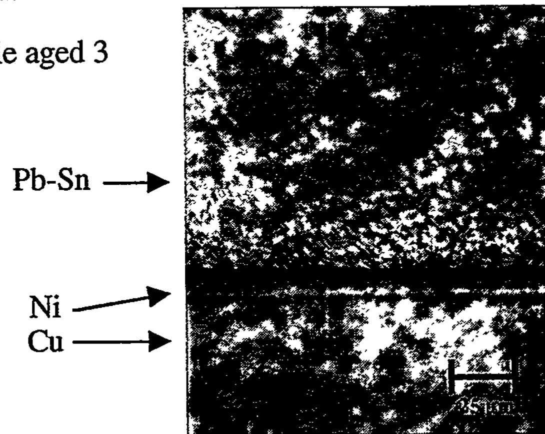

Figure 3.2.4b- Sample aged 3 days at 150 °C, and then reflowed again

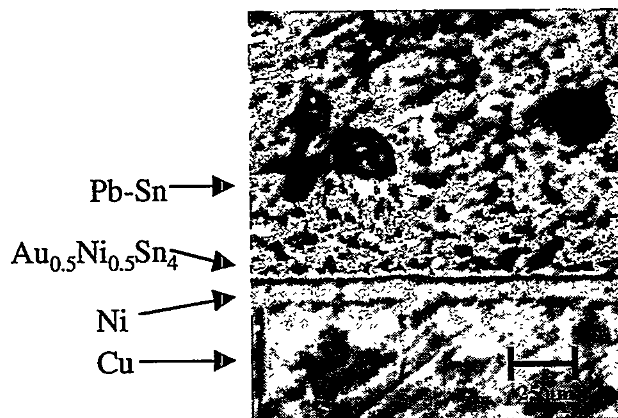

Figure 3.2.4c- Sample aged 3 days at 150 °C, reflowed again, and then aged for another 3 days